

# How the Counterion Affects Ground- and Excited-State Properties of the Rhodopsin Chromophore

Julia Hufen,<sup>†</sup> Minoru Sugihara,<sup>\*,‡</sup> and Volker Buss<sup>†</sup>

*Institute of Theoretical Chemistry and Institute of Theoretical Low-Temperature Physics,  
University of Duisburg-Essen, D47048 Duisburg, Germany*

*Received: August 26, 2004; In Final Form: September 28, 2004*

High-level DFT and ab-initio CASSCF/CASPT2 methodologies have been applied to study the ground and excited states of the retinal chromophore as a function of counterions of different complexities. On the basis of the recent 2.8 Å X-ray structure of rhodopsin, the complete retinal chromophore was optimized in the presence of anionic Glu113, Thr94, and a water molecule (Wat2b), which together form a complex counterion of the protonated Schiff base. In addition, complexes were studied in which components of the counterion (Thr94 and/or Wat2b) were removed and also the free chromophore without any counterion, both in the protonated and deprotonated forms; for the CASSCF/CASPT2 calculations a reduced model chromophore with five conjugated double bonds was employed. In the presence of any counterion, bond alternation increases strongly in the region close to the Schiff base nitrogen, resulting in a structure similar to the protonated Schiff base. There is a conspicuous reduction in bond alternation in the three bonds from C9 to C12, which is already visible in the structure of the bare protonated chromophore. Comparison with other methods shows that bond alternation is exaggerated whenever noncorrelated theoretical methods are employed and may be exaggerated by the experimental methods as well. Bond alternation affects the excited-state energies only slightly. The large blue shift which the counterion exerts on the strongly allowed S<sub>1</sub> state of the chromophore is caused mainly by the charge of the counterion against which the electron density of the excited state is shifted. The effect of the counterion on the S<sub>2</sub> state is small. This agrees with the calculated electric dipole moment of the chromophore upon excitation to S<sub>1</sub> and S<sub>2</sub> which changes strongly in magnitude and direction in the S<sub>1</sub> state but is hardly affected when the S<sub>2</sub> state is involved.

## 1. Introduction

Rhodopsin is the membrane protein that is responsible for dark/light vision in the vertebrate eye where it is present in high concentrations in the rod cell outer segments. Activation of the protein by light is mediated by the chromophore, 11-*cis*-retinal, which is covalently bound via a protonated Schiff base linkage to the  $\epsilon$ -amino group of Lys-296. When light in the visible region hits the chromophore, photoisomerization of the 11-*cis*-bond to trans takes place with the chromophore adopting a highly twisted conformation.<sup>1</sup> The geometry change of the chromophore is then transmitted into a change of the protein conformation, activation of the intracellular surface toward coupling with the heterotrimeric G-protein transducin, and initiation of the visual cascade.<sup>2,3</sup>

Rhodopsin is the first G-protein coupled receptor (GPCR) whose crystal structure was solved by X-ray analysis.<sup>4</sup> Since then the 2.8 Å resolution of that study has been gradually improved. Water molecules have been located in the 2.6 Å structure, two of them close to the binding site,<sup>5</sup> and the complete polypeptide chain has been resolved in the most recent 2.2 Å structure.<sup>6</sup> The electron density map reveals in marked detail how the chromophore in its twisted 6-*s-cis*-11-*cis* configuration is embedded in the binding pocket provided by the 7-transmembrane helix bundle of the protein.

One of the most remarkable features of rhodopsin concerns the absorbance of the chromophore. Visual pigments of different species absorb at different wavelengths, a prerequisite for survival in different habitats.<sup>7</sup> In the same species pigments may show varying sensitivity in the regions of the electromagnetic spectrum, which is the basis for color vision.<sup>8</sup> Finally, shifts of the absorption maximum are observed as the protein passes through the different intermediates of the photocycle,<sup>9</sup> making the chromophore an ideal indicator of the molecular environment in which it is embedded. A convenient measure of these spectral changes is the so-called opsin shift, which is the displacement of the chromophore absorption maximum in the pigment relative to its absorption in an isotropic solvent such as methanol. Despite numerous efforts,<sup>10–27</sup> a comprehensive picture of the different factors contributing to the opsin shift is still missing.

In a number of recent studies we applied a nonempirical quantum-mechanical scheme, CASPT2, to show how conformational changes of the chromophore, in particular nonplanar deformations of the unsaturated chain, change the spectral properties of the retinal chromophore in rhodopsin and in the first photoproduct, bathorhodopsin.<sup>26,27</sup> We report now how the interaction between the retinal Schiff base and its complex counterion affects the structure of the chromophore in its ground state and its excitation into low-lying excited states. These calculations are purely nonempirical, i.e., both the chromophore and its environment are treated by high-level quantum mechanics only, which limits the study to a minimal model consisting of a reduced chromophore and the counterion complex. Effects of

\* To whom correspondence should be addressed. Phone: +49–203 379 1073. Fax: +49–203 379 3665. E-mail: minoru@thp.uni-duisburg.de.

<sup>†</sup> Institute of Theoretical Chemistry.

<sup>‡</sup> Institute of Theoretical Low-Temperature Physics.

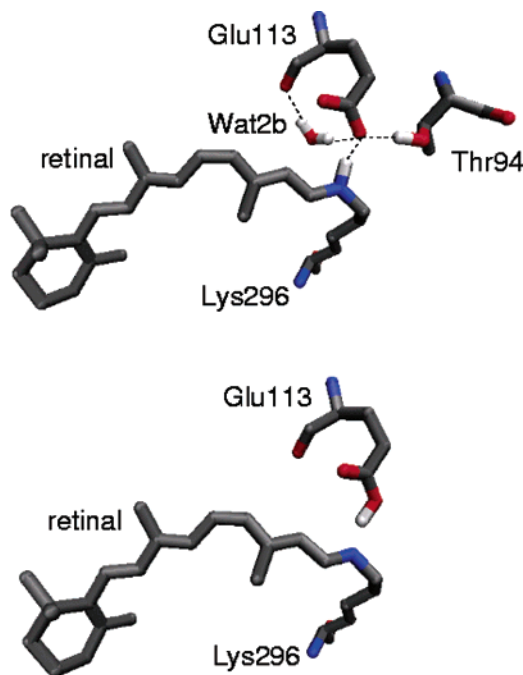


**Figure 1.** Structures of the protonated 11-*cis*-retinal Schiff base complex with the complete counterion, **pSb1** (top), and the deprotonated Schiff base with glutamic acid only, **Sb1** (bottom). Not shown are the intermediate complexes in which either Wat2b (**pSb2**) or Thr94 (**pSb3**) is removed and the bare chromophores, **pSb** and **Sb**.

other charges and of polarizable groups close to the chromophore cannot be considered at this level of theory. The calculations show that there is considerable bond alternation along the conjugated chain regardless of the nature of the counterion and the protonation state of the chromophore. This alternation is exaggerated by all methods employing uncorrelated wave functions and apparently also by the experimental methods. There is reduced bond alternation in the region from C9 to C12. The effect of bond alternation on the excited-state energies is small: the large blue shift of the strongly allowed  $S_1$  excitation in the presence of the counterion is mainly a result of the electrostatic interaction between the negatively charged Glu113 residue and the excited-state charge distribution of the chromophore.

## 2. Models and Computational Methods

We optimized the ground state of the retinal chromophore in the presence of the complex counterion shown as **pSb1** in Figure 1. In this complex the negatively charged Glu113 acts as the primary counterion, forming a salt bridge with the positively charged Schiff base nitrogen of the chromophore. This bridge is stabilized by hydrogen bonds involving Glu113 and the polar side groups of Thr94 (and probably Ser186, not shown here) and by coordination of a water molecule (Wat2b). Also optimized were structures in which components of the counterion were removed: **pSb2** and **pSb3**, in which Wat2b or Thr94 were omitted, respectively. These complexes have been shown by molecular dynamics (MD) simulations to render the chromophore less stable toward deprotonation.<sup>28,29</sup> When both Wat2b and Thr94 are removed leaving only Glu113 to neutralize the positive charge of the chromophore, the minimal complex **Sb1** is obtained which, however, is not stable in the charge-separated form and rapidly converts into the neutral Schiff base/glutamic acid pair. Also included in the study were **pSb** and **Sb**, which refer to the bare protonated and deprotonated 11-*cis*-retinal

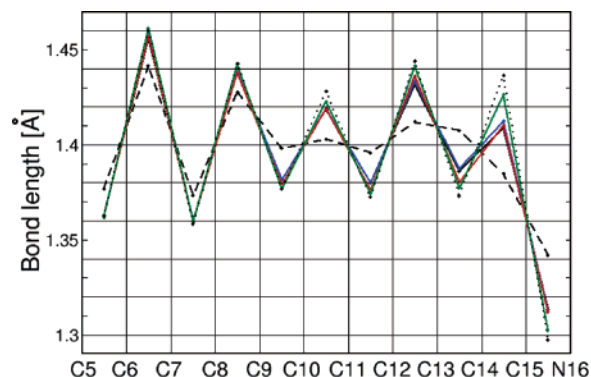


**Figure 2.** Bond lengths of the retinal chromophore optimized with VASP in the presence of different counterions: **pSb1** (in black), **pSb2** (blue), **pSb3** (red), and **Sb1** (green). The bare protonated (**pSb**) and deprotonated (**Sb**) Schiff bases are shown in dashed and dotted black lines, respectively.

Schiff base, respectively, optimized in vacuo in the absence of any counterion.

These complexes were geometry optimized with the Vienna Ab Initio Simulation Package (VASP), a density functional theory (DFT) based MD program<sup>30</sup> starting with the chromophore of the 2.8 Å crystal structure.<sup>4</sup> It uses a plane wave basis set and Vanderbilt–Kresse ultrasoft pseudopotentials. Details about the program can be found in the literature.<sup>30</sup> Geometry optimization renders the chromophore essentially planar, with only the C6–C7 bond significantly twisted. This is a consequence of the missing protein pocket which is known to induce the twisted C11–C12 conformation in the protein.<sup>31</sup> For the calculations we employed periodic boundary conditions with a supercell of sufficient size to exclude the interaction with image molecules. In the model the complete amino acids were considered including the peptide backbone, beyond which the bonds were cut and saturated with hydrogen atoms. The geometry minimization was performed with only the peptide backbone atoms of the amino acids fixed; all other nuclei were allowed to move without constraints. More information about the parameters applied can be found in two recent articles.<sup>28,29</sup>

For the calculation of ground- and excited-state energies we employed the CASSCF/CASPT2 method as provided by the MOLCAS5 set of routines.<sup>32</sup> With this method ab initio multiconfigurational wave functions are computed and combined with second-order perturbation theory for specified states.<sup>33,34</sup> State-averaged wave functions are expanded in a set of atomic natural orbitals (ANO)<sup>35,36</sup> consisting of 4s3p1d for carbon, nitrogen, and oxygen and 2s for hydrogen. This basis set yields highly accurate energies for cationic  $\pi$ -systems<sup>37,38</sup> and has been used for the calculation of rhodopsin model chromophores before.<sup>26,27</sup> We calculated six states for **pSb**, **pSb1**, **pSb2**, and **pSb3** and eight states for **Sb** and **Sb1**. The latter were recalculated with six states, and little differences were found for the state configurations calculated with the two approximations. CASPT2 is very time-consuming and requires huge amounts of disk space for storage of intermediate integrals. The complete 11-*cis*-retinal chromophore plus the complex counterion exceed the limits set by the present hardware, and thus, the following measures had to be taken: the  $\beta$ -ionone ring with its double bond was cut off, leaving the chromophore 5-*Z*-4,8-dimethyl-nona-3,5,7,9-tetraeneimine. Also, the complex counterion was reduced to the functional groups. Thus, Glu113 was reduced to formic acid ( $\text{HCOO}^-$ ) or formate ( $\text{HCOOH}$ ) depending on the protonation state, and Thr94 with its polar side group was reduced to a water molecule; Lys296 was left out completely. Free valencies where the bonds were cut were

**TABLE 1: CASSCF- and CASPT2-Corrected State Energies  $E$ ,<sup>a</sup> Oscillator Strengths  $f$ , Main Contributing Configurations<sup>b</sup> with Weights (in *italics*, %) for the Ground and the Excited States, and Dipole Moments<sup>c</sup>**

complex	$E$ (CASSCF)	state	$E$ (CASPT2)	$f$	configuration (CASPT2)	dipole moment			
						x	y	z	m
<b>pSb</b>	−481.2333	S <sub>0</sub>	−481.7584		(4a) <sup>2</sup> (5a) <sup>2</sup> 80	−3.87	2.22	−0.04	11.35
	2.96 (418)	S <sub>1</sub>	2.39 (519)	1.34	(5a) <sup>1</sup> (6a) <sup>1</sup> 67	0.05	2.28	−0.10	5.80
	3.48 (357)	S <sub>2</sub>	3.01 (412)	0.04	(5a) <sup>1</sup> (7a) <sup>1</sup> 14	−3.74	2.13	−0.05	11.00
					(4a) <sup>1</sup> (6a) <sup>1</sup> 25				
<b>pSb1</b>	−820.7781	S <sub>0</sub>	−823.2769		(5a) <sup>0</sup> (6a) <sup>2</sup> 26				
	5.10 (243)	S <sub>1</sub>	3.18 (390)	0.93	(4a) <sup>2</sup> (5a) <sup>2</sup> 68	2.65	2.51	0.03	9.27
	3.77 (329)	S <sub>2</sub>	3.32 (374)	0.01	(5a) <sup>1</sup> (6a) <sup>1</sup> 54	6.82	2.56	−0.05	18.52
					(5a) <sup>1</sup> (7a) <sup>1</sup> 14	2.75	2.38	0.04	9.23
<b>pSb2</b>	−744.7270	S <sub>0</sub>	−747.0087		(4a) <sup>1</sup> (6a) <sup>1</sup> 18				
	5.21 (238)	S <sub>1</sub>	3.12 (398)	0.98	(5a) <sup>0</sup> (6a) <sup>2</sup> 32	2.51	2.71	1.11	9.81
	3.80 (327)	S <sub>2</sub>	3.34 (371)	0.01	(4a) <sup>2</sup> (5a) <sup>2</sup> 68	6.91	2.73	1.14	19.10
					(5a) <sup>1</sup> (6a) <sup>1</sup> 66	2.64	2.59	1.13	9.83
<b>pSb3</b>	−744.7303	S <sub>0</sub>	−747.0130		(5a) <sup>1</sup> (7a) <sup>1</sup> 14				
	5.20 (239)	S <sub>2</sub>	3.11 (399)	0.96	(4a) <sup>1</sup> (6a) <sup>1</sup> 18	0.81	2.62	−0.30	7.00
	3.70 (335)	S <sub>3</sub>	3.25 (382)	0.01	(5a) <sup>0</sup> (6a) <sup>2</sup> 32	4.97	2.65	−0.33	14.33
					(4a) <sup>2</sup> (5a) <sup>2</sup> 75	0.99	2.47	−0.29	6.81
<b>Sb1</b>	−668.7013	S <sub>0</sub>	−670.7567		(4a) <sup>1</sup> (6a) <sup>1</sup> 17				
	5.27 (235)	n− $\pi^*$	4.48 (277)	0.00	(5a) <sup>0</sup> (6a) <sup>2</sup> 32	0.53	1.45	0.37	4.04
	5.87 (211)	S <sub>2</sub>	3.47 (357)	0.99	(n) <sup>2</sup> (4a) <sup>2</sup> (5a) <sup>2</sup> 75	−1.08	0.97	0.49	3.89
	3.90 (318)	S <sub>3</sub>	3.48 (356)	0.00	(n) <sup>1</sup> (5a) <sup>2</sup> (6a) <sup>1</sup> 73	2.71	1.41	0.30	7.82
<b>Sb</b>	−479.8747	S <sub>0</sub>	−481.3806		(n) <sup>2</sup> (5a) <sup>1</sup> (6a) <sup>1</sup> 70	0.66	1.39	0.39	4.03
	4.51 (275)	n− $\pi^*$	3.94 (315)	0.00	(n) <sup>2</sup> (4a) <sup>1</sup> (6a) <sup>1</sup> 18				
	6.16 (201)	S <sub>2</sub>	3.80 (326)	1.02	(n) <sup>2</sup> (5a) <sup>0</sup> (6a) <sup>2</sup> 31	0.51	0.67	−0.01	2.13
	4.04 (307)	S <sub>1</sub>	3.62 (342)	0.00	(n) <sup>2</sup> (4a) <sup>2</sup> (5a) <sup>2</sup> 76	−0.87	0.49	0.04	2.55
					(n) <sup>1</sup> (5a) <sup>2</sup> (6a) <sup>1</sup> 74	1.40	0.67	−0.02	3.94
					(n) <sup>2</sup> (5a) <sup>1</sup> (6a) <sup>1</sup> 70	0.60	0.63	−0.01	2.22
					(n) <sup>2</sup> (5a) <sup>1</sup> (7a) <sup>1</sup> 15				
					(n) <sup>2</sup> (4a) <sup>1</sup> (6a) <sup>1</sup> 19				
					(n) <sup>2</sup> (5a) <sup>0</sup> (6a) <sup>2</sup> 31				

<sup>a</sup> For the S<sub>0</sub> state, absolute energy in au. For the other states, relative energies in eV and nm (in parentheses). <sup>b</sup> For the ground state the two highest occupied orbitals are tabulated. For the excited states only holes and electrons created. <sup>c</sup> x-, y-, and z-components in au. The moment is in Debye.

saturated with hydrogen atoms. Substituting the reactive groups for the amino acids will hardly affect the calculated spectroscopic properties but leaves the hydrogen-bonding network intact. Still, more than 18 Gbyt hard disk space and 1 Gbyt memory are required for the calculation of this reduced model chromophore with five conjugated double bonds.

The active space included 10 electrons in 10 orbitals, i.e., all pseudo- $\pi$ -electrons and valence pseudo- $\pi$ -orbitals were considered. For the nonprotonated structures **Sb** and **Sb1** we also calculated the n− $\pi^*$  transitions. For this the active space was enlarged by the n orbital, so that the active space consisted of 12 electrons and 11 orbitals. All core orbitals were kept frozen during the CASPT2 calculations, and the level shift to avoid the effect of intruder states was set to 0.3 au. To obtain oscillator strengths, the CASPT2-corrected state energies were combined with transition dipole moments calculated by the CAS state interaction method (CASSI).<sup>39</sup>

### 3. Results

#### Geometries.

The protein pocket affects the chromophore geometry mainly in two ways. One is the nonplanar distortion of the conjugated chain in the central region, from C10 to C13, which is induced by steric and/or electronic effects of the protein environment.<sup>31</sup> This distortion has been discussed in connection with the selective and extremely rapid photoisomerization about the C11–C12 bond of rhodopsin.<sup>40–42</sup> The other concerns the counterion which tends to localize the positive charge of the conjugated Schiff base chromophore at the imine nitrogen,

leading to double-bond fixation and bond length alternation along the unsaturated chain.<sup>43,44</sup> Only the latter effect, and how it will change the absorbance of the chromophore, is the topic of this paper.

Figure 2 shows the bond lengths of the chromophore without external charge and in the presence of four different counterions. The energy-optimized position of the counterion is about 2.6 Å from the nitrogen atom, a distance which is significantly less than that found in the current X-ray structures (3.2 Å).<sup>4–6</sup> The pattern of alternating bond lengths which corresponds to the valence bond structure of the conjugated  $\pi$ -system is clearly visible. The limiting cases of weak and strong bond alternation are realized by the bare protonated Schiff base **pSb** and the deprotonated Schiff base **Sb**, respectively. In the former, carbon–carbon bond lengths are rather similar from C15 to C9, regardless of whether they pertain to formal single or double bonds, while at larger distances from the positive center, starting with the C8–C9 single bond, significant bond alternation sets in. In the deprotonated Schiff base, on the other hand, there is strong bond alternation throughout the conjugated chain. In the presence of any counterion the bond alternation of the Schiff bases become similar to the bare deprotonated chromophore, with differences observable only in the vicinity of the azomethine nitrogen, up to and including C9. In this region bond alternation is visibly smaller in the charged complexes **pSb1**, **pSb2**, and **pSb3** and also in the neutral complex **Sb1** compared to **Sb**. The different stability of the complexes against deprotonation of the chromophore, which was deduced on the basis



of DFT MD simulations, is not reflected in significant structural differences of the chromophore.

In contrast to the nonplanar distortions of the chromophore which have been discussed ever since the first X-ray structure of bovine rhodopsin appeared,<sup>4</sup> bond alternation has not been such a relevant topic. In fact, the term does not even appear in the first three publications presenting structures with increasing resolution.<sup>4,5,45</sup> However, perusal of the coordinate lists reveals that in all these structures the chromophore exhibits significant bond alternation, a consequence probably of the refinement of the diffraction data with theoretical methods. Comparison with different experimental data sets<sup>6</sup> reveals that for the section covered by our model chromophore the “best” set of bond lengths calculated on the basis of experimental structures agrees very well with the present results given in Figure 2. This should be not too surprising considering that the same theoretical (DFT) methodology has been employed; it shows, on the other hand, that in contrast to the nonplanar distortions of the chromophore, the bond length pattern is primarily an intrinsic property of the chromophore modulated by the counterion.

### Excited States.

In Table 1 the calculated ground- and excited-state energies, oscillator strengths, CASPT2 configurations, and ground- and excited-state dipole moments are listed for the six chromophore complexes. Note that these are pure quantum-mechanical results in which the environment, i.e., the complex counterion, is treated as an integral part of the chromophore. Perusal of the table reveals that the calculations are internally consistent and yield a useful classification of the different states.

The ground state is mainly closed shell in all cases, with 68–80% contribution from that configuration,  $5a^26a^0$ . With a calculated dipole moment of 11.35 D, the charge distribution is highly unsymmetrical for the free protonated Schiff base. With the negatively charged counterion the dipole moment is reduced as expected; a strong reduction is observed upon deprotonation as there are no longer any formal charges.

The excited state with high oscillator strength ( $f \geq 0.93$ ) always involves, with weights ranging from 54% to 70%, the HOMO to LUMO configuration ( $5a^16a^1$ ). This is the state which is lowered most in energy relative to the ground state by the CASPT2 treatment, averaging 2 eV in all complexes except **pSb**, where the energy gain is less than 0.6 eV. For simplicity of formulation, we will refer to this state—which is the lowest excited energy state in all complexes except **pSb3**, **Sb1**, and **Sb** where it is  $S_2$ —as the  $S_1$  state in the following discussion. Excitation into  $S_1$  is associated with a strong change of the dipole moment, both in magnitude and in orientation (see below).

The next higher state  $S_2$  ( $S_3$  in **pSb3** and **Sb1** and  $S_1$  in **Sb**) is mostly doubly excited HOMO to LUMO ( $5a^06a^2$ ) plus equal contributions of HOMO-1 to LUMO ( $4a^16a^1$ ) and HOMO to LUMO+1 ( $5a^17a^1$ ) excitation. The perturbational treatment lowers the energy of this state by, on average, only 0.45 eV. There is no intensity in this state, and the dipole moment is almost identical to the ground state.

Finally, in the complexes with a deprotonated chromophore (**Sb** and **Sb1**) there should be an additional  $n-\pi^*$  excitation ( $n^16a^1$ ) which is found close in energy to the  $S_1$  state in the free Schiff base (**Sb**) but is strongly blue shifted in the presence of the (uncharged) counterion (**Sb1**).

A summary of the CAS and the CASPT2 calculated  $S_1$ ,  $S_2$ , and  $n-\pi^*$  energies relative to  $S_0$  is shown in Figure 3. In **pSb**, the lowest excited state according to the CAS treatment is  $S_1$ ; the  $S_2$  state is about 0.5 eV higher in energy. CASPT2 shifts

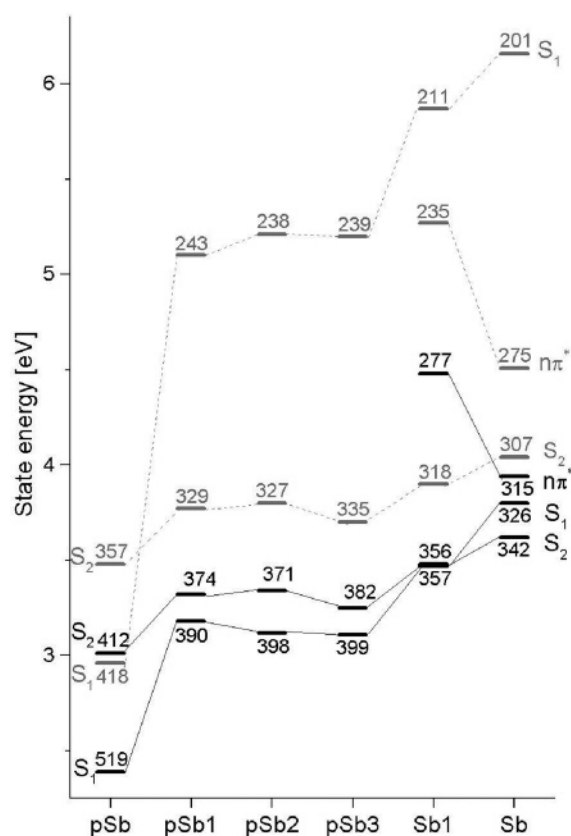


**Figure 3.** CAS (in gray) and CASPT2 (in black) calculated excited-state energies relative to the ground state of the retinal chromophore model in the presence of different counterions. The numbers on the energy levels are excitation energies in nm.

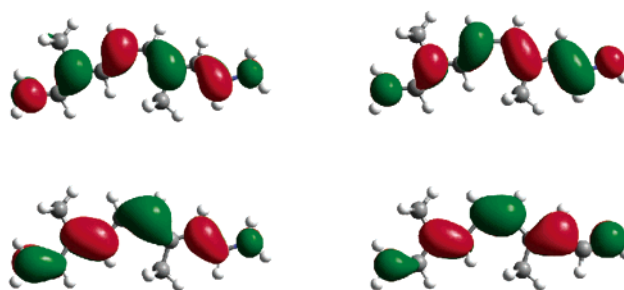


**Figure 4.** LUMO (top) ( $\pi_5$ ) and HOMO (bottom) ( $\pi_6$ ) of the bare protonated Schiff base **pSb** (left) and the deprotonated Schiff base **Sb** (right).

both states to lower energies by roughly the same amount, 0.5 eV. The figure reveals how the (CASPT2 calculated) difference between the  $S_1$  and  $S_2$  states decreases in the presence of charged counterions until they become degenerate in **Sb1**. Finally, in the free deprotonated Schiff base the “forbidden”  $S_2$  state drops below the  $S_1$  state. The reason for this state inversion is the large destabilization of the  $S_1$  state relative to  $S_2$  at the CAS level, which is only partially reversed in the PT2 treatment.

Despite the terminal substitution by the NH group, the electronic structure of the deprotonated Schiff base **Sb** is very similar to a conjugated polyene. The isoelectronic 1,3,5,7,9-decapentaen absorbs at 336 nm,<sup>46</sup> remarkably close to the calculated 326 nm for the  $S_1$  state of the Schiff base. The state inversion of  $S_1$  and  $S_2$  is also established for long polyenic systems: in 1,3,5,7-octatetraene, the largest polyene for which exact CASPT2 calculations are available,<sup>47</sup> the lowest excited state is the forbidden  $2^1A_g$  state which corresponds to the  $S_2$  state in **Sb**. The strongly allowed  $1^1B_u$  state is calculated to be

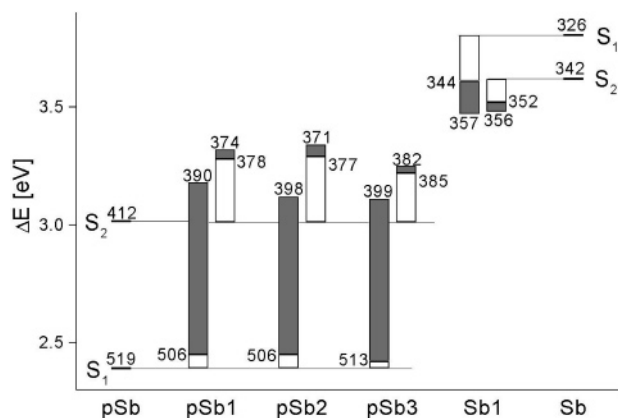


**Figure 5.**  $S_1$  and  $S_2$  energy changes of the different chromophore complexes due to geometry changes (white bars) and the charge of the counterion (gray bars).

15 nm higher in energy with the difference expected to increase as the chain gets longer.

The calculated  $S_1$  energy in **pSb** is significantly lower than that in **Sb**. With 519 nm the absorption maximum of this cationic dye with one terminal nitrogen atom is right in the middle of two completely delocalized but symmetrical dye cations with the same number of  $\pi$ -electrons: the polyenyl cation with carbon atoms only along the unsaturated chain (528 nm)<sup>38</sup> and the heptamethine cyanine dye with two terminal nitrogen atoms (484 nm).<sup>37</sup> In both the polyenyl and the cyanine dye the  $S_2$  state is strongly blue shifted relative to  $S_1$ , as found also in the protonated Schiff base **pSb**.

We conclude that both with respect to ground-state geometries and excited-state energies the deprotonated and free protonated Schiff bases, **Sb** and **pSb**, present limiting cases in the spectrum of unsymmetrically substituted conjugated  $\pi$  systems, the former with largely localized double bonds and polyenic excited-state properties and the latter with largely delocalized double bonds and cyanine-like properties. The gap between the two is bridged by the counterion complexes.

The difference between the two types of  $\pi$  systems embodied by **Sb** and **pSb** is also evident from the shape of the orbitals which are mainly involved in the  $S_0$  to  $S_1$  excitation: the highest occupied and the lowest unoccupied orbitals,  $\pi_5$  and  $\pi_6$ , respectively, shown in Figure 4.  $\pi_5$  of the Schiff base **Sb** is typical polyenic, with the five electron density maxima located at alternating bonds, leading to the observed double-bond fixation. The corresponding orbital in **Sb1** is distorted due to the positively charged nitrogen which pulls electron density into the less attractive single-bond regions between C12 and C13 and between C14 and C15. As a consequence of this deformation (which is also seen in the a conjugation defect centered at C12), the double bonds increase and the single bonds decrease in lengths relative to the deprotonated Schiff base.

#### Effect of the Counterion.

The effect of the counterion on the chromophore is 2-fold: it localizes the positive charge on the Schiff base nitrogen, thereby increasing bond alternation. Second, as a result of the electronic excitation charge density it is shifted along the chromophore and stabilized or destabilized in the presence of the negatively charged counterion depending on the direction of this shift. For an estimate of the relative importance of these two effects, we repeated the CASPT2 calculations for a hypothetical intermediate state in which only the geometry change of the chromophore due to the counterion is considered but not the counterion itself. The results for the  $S_1$  and  $S_2$  states are shown in Figure 5. For the protonated Schiff bases **pSb1**—

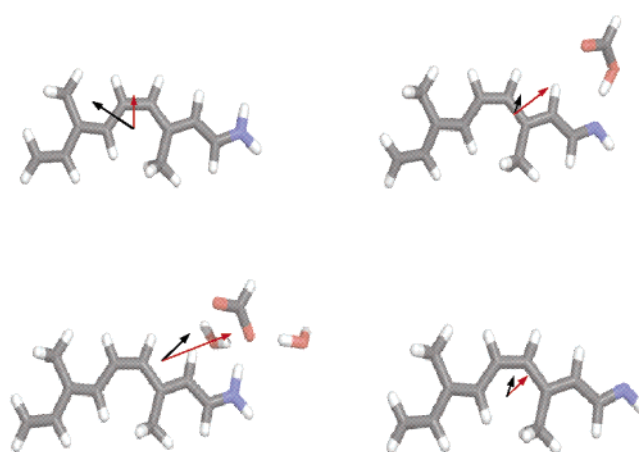


**Figure 6.** Dipole moments of the  $S_0$  (black arrows) and the  $S_1$  states (red arrows) of **pSb** and **pSb1** (left column) and **Sb1** and **Sb** (right column). Note: contrary to convention, the direction of the dipole has been chosen to point from the center of the positive to the center of the negative charge.

**pSb3**, the counterion-induced shift of the  $S_1$  state can be seen to be almost entirely due to the charge of the counterion; the effect of the geometry change is considerably less (ca. 0.1 eV of a total of more than 1 eV). For the  $S_2$  state, the relative importance of the two effects is opposite though smaller as a whole: the major part of the blue shift is due to the counterion-induced geometry change, while the effect of the counterion charge is almost nil. For the neutral complex **Sb1**, it is convenient to choose the deprotonated Schiff base **Sb** as a point of reference. In this case there is no formal charge but only the interaction with the dipole moment of the glutamic acid. In this case both the  $S_1$  and  $S_2$  states are stabilized by the geometry changes and in addition by the dipolar charge distribution of the glutamic acid residue.

This interpretation is supported by the changes of the charge distribution which take place when upon excitation the chromophore is promoted into an excited state. In Figure 6 the ground state and the  $S_1$  excited-state electric dipole moments are sketched for the protonated and deprotonated chromophore in both the presence and the absence of a counterion. Note that contrary to general usage, the arrowhead of the moment vectors points toward the center of the negative charge, with the origin fixed in the center of the nuclear framework. According to Table 1 the dipole moments of the  $S_2$  states are virtually identical to the  $S_0$  states in all complexes studied, so we have not included those moments in the figure. The basic pattern is the same in the four complexes shown: there is a shift of negative charge toward the positive Schiff base nitrogen as the chromophore is excited into the  $S_1$  state, and this shift is significantly larger when the chromophore is protonated. From electric field-induced changes of the absorption spectra, Mathies et al. concluded<sup>48,49</sup> that there is a large change of the dipole moment as the chromophore becomes electronically excited, an effect which is probably enhanced in the condensed phase where the high polarizability of the excited state leads to a strongly increased excited-state moment. It is interesting to note that the change of the dipole moment from  $S_0$  to  $S_1$  is identical in **pSb** and **pSb1**, which is another indication that the major effect of the counterion on the chromophore is electrostatic and involves only minor changes of the wave function.

#### 4. Discussion

Control of the protonation state of the retinal chromophore is of critical importance for the chain of events going from the

initial capture of a photon in the dark state conformation of rhodopsin to the signaling state where rhodopsin couples with the G-protein and starts the visual cascade: only the protonated chromophore absorbs at wavelengths in the “visible” region, while deprotonation or neutralization of the chromophore appears to be required to reach the active state, destroying what has been called one of the crucial stabilizing elements of the ground state of the protein.<sup>3</sup> We have shown recently<sup>28,29</sup> how the unique coordination of Glu113 with the polar side group Thr94 and a water molecule makes the counterion sufficiently acidic to keep the chromophore protonated. To this arrangement should be added the interaction with Ser186, which completes the chain of hydrogen bonds extending to Glu181, which is also discussed in connection with the so-called counterion switch possibly taking place when the active state of the protein is reached.<sup>50,51</sup>

In addition to the fact that a strong acid is needed to stabilize the protonated state of the chromophore<sup>52,53</sup> there are consequences resulting from the peculiar disposition of the charged counterion with respect to the chromophore. Bond alternation of the protonated retinal Schiff base in the ground state is undisputed from both experimental and theoretical evidence, but there is no agreement about the magnitude of bond alternation or how bond alternation might affect the reactivity of the chromophore. Bond lengths of the all-*trans*-retinal Schiff base chromophore in bacteriorhodopsin have been calculated by Vreven and Morokuma<sup>24</sup> using embedded quantum-mechanics (QM/MM) schemes with both *ab initio* Hartree–Fock (HF) and DFT methodology for the QM part. Their results are comparable to ours when DFT is employed; with HF theory bond alternation increases strongly. Ferre and Olivucci<sup>25</sup> using CASSCF methodology in addition to an AMBER force field to find much stronger bond alternation than we do. The distance between the counterion and the chromophore in the structural model used in that study is significantly larger (3.7 Å) than that in ours, which if anything should reduce, not increase, the degree of bond alternation.

HF theory is known to overemphasize double-bond fixation because of its bias toward electron pairing and its neglect of correlation effects.<sup>24,54</sup> This inherent drawback, which is avoided in DFT by an appropriate choice of the exchange integral, can only be remedied by a post-HF treatment such as second-order Møller–Plesset theory (MP2). We are not aware of any geometry optimization at the CASPT2 level, certainly not of a system as large as retinal. Consequently, we optimized the all-*trans*-penta-3,4-dieneiminium cation with a 6-31G\* basis set employing five different methods, restricted HF (RHF), RHF-MP2, CASSCF, CASPT2, and B3LYP-DFT, and found an almost identical distribution of bond lengths for the correlated methods (RHF-MP2 and DFT) and for CASPT2. In contrast, CASSCF theory gives double-bond lengths which are on average 0.2 Å shorter and single-bond lengths which are 0.2 Å longer than the corresponding correlated values. It appears that the limited space in which the excited configuration state functions in the CASSCF treatment are expressed is not of sufficient size to remedy the correlation error inherent in the HF method.

Experimentally, bond alternation of a magnitude comparable to the CASSCF calculations<sup>25,55</sup> (and much stronger than calculated by us) was found in a recent investigation of the retinal chromophore in rhodopsin by double-quantum solid-state

NMR spectroscopy.<sup>56</sup> One particular result of the experimental study is the conspicuous decrease of bond alternation in the region from C11 to C14, which was attributed to penetration of the positive charge of the chromophore into that region brought about possibly by the perturbation of the chromophore by the water molecule close to C12. In a related theoretical study<sup>57</sup> this reduced bond alternation of the retinal chromophore was brought about by the negative charge of an acetate group positioned off the chromophore plane right next to C12, a geometry which is not substantiated by any of the experimental structures. Decreased bond alternation in the isomerization region is also manifest in our calculations (see Figure 2), where, however, we excluded any special effect by the environment (the only water molecule in our complex is coordinated to Glu113). Our rationale for the observed effect is documented in Figure 4 and relies on the peculiar shape of the HOMO. In this orbital the five antinodes are attracted to the positive potential of five double bonds, on one hand (leading to the strong bond alternating structure of the neutral Schiff base shown in the same Figure), and to the positive terminus of the imine nitrogen, which leads to the calculated structural defect of this orbital from C11 to C13. More work is clearly needed to elucidate whether the counterion plays any role in the extremely fast, efficient, and selective photoisomerization of the chromophore.

With respect to the excited-state energy, the role of the counterion seems to be less controversial. The protonation state of the chromophore is the single most efficient factor that determines the absorbance of the rhodopsin chromophore. In fact, a long-wavelength absorption maximum that may during the photocycle of rhodopsin ( $\lambda_{\text{max}} = 500$  nm) shift to 570 nm in photorhodopsin and 478 nm in metarhodopsin I (corresponding to energy differences of 0.1 and 0.3 eV, respectively) is a definite sign for a protonated chromophore and by conjecture the presence of a counterion. The transition from meta I to meta II, in contrast, is accompanied by a much larger shift (102 nm or 0.67 eV), which is comparable in magnitude to the blue shift that a protonated retinal Schiff base undergoes upon deprotonation in a bulk solvent and is evidence that the salt bridge between the counterion and the chromophore is broken and that neutralization has taken place.

Perusal of Figure 5 indicates that the distinction between the two protonation states may not be that simple. Deprotonation of the bare chromophore shifts the  $S_0$  to  $S_1$  excitation from 519 to 326 nm (some 1.4 eV). However, in the presence of a counterion, i.e., when deprotonation involves transfer of the proton from the chromophore to Glu113, this shift is reduced to only 0.3 eV (**pSb1** to **Sb1**). This means that deprotonation of the chromophore covalently bound by the lysine side chain may involve wavelength changes of as little as 30–40 nm in the UV–vis spectrum. Thus, the observed shift from 478 to 380 nm in the meta I to meta II conversion of rhodopsin might be indicative of larger structural rearrangements than a simple proton-transfer reaction from the chromophore to the counterion.

## 5. Conclusions

On the basis of model structures which were minimized by an *ab initio* plane wave code, we studied the geometry and optical properties of the retinal chromophore in the presence of different counterions at the CASSCF and CASPT2 level of theory. Our main conclusions are as follows.

(i) In the presence of any counterion, the chromophore displays significant bond alternation which is reduced somewhat



in the region from C9 to C12. This reduction is most visible in the bare protonated chromophore and is caused by a conjugation defect of the HOMO. Bond alternation is exaggerated in all noncorrelated quantum-mechanical methods and in the CASSCF method with the conventional choice of active space. Bond alternation may be exaggerated also in the refined X-ray structures.

(ii) The highly allowed  $S_1$  state is strongly blue shifted in the presence of the counterion; the shift is mainly a consequence of negative charge being moved toward the counterion as a result of electronic excitation. The effect of the counterion on the  $S_2$  state is much smaller; also, there is no change of the dipole moment as the chromophore is excited into this state. In the neutral chromophore complex both the  $S_1$  and  $S_2$  states are stabilized in the presence of the (neutral) counterion. As a result of these opposing effects, proton transfer from the chromophore to the counterion is significantly reduced and may involve energies of as little as 0.3 eV.

Our conclusions are preliminary and may change as the model is enlarged and more structural information becomes available. This concerns, in particular, the distance between the chromophore and counterion on which the spectroscopic shifts depend most strongly: a larger distance between the counterion and chromophore will shift the neutral complex toward **Sb** and the charged complex toward **pSb**, thereby increasing the energy difference between the  $S_1$  states. In our calculations we used throughout the optimized N–H–O bridge distance of 2.6 Å; experimentally, the value found is closer to 3.2 Å.<sup>4–6</sup> More work is clearly needed before definite statements can be made regarding the effects of the counterion on the properties of the rhodopsin chromophore.

**Acknowledgment.** We thank Oliver Weingart for the CASPT2 optimization and Marko Schreiber for discussion. This work is supported by the Graduated School on Structure and Dynamics of Heterogeneous Systems at the University of Duisburg-Essen and the Research Group Molecular Mechanisms of Retinal Protein Action, both financed by the Deutsche Forschungsgesellschaft. We thank the Regional Computer Center of the University of Cologne for generous computational resources.

**Supporting Information Available:** Cartesian coordinates of all optimized structures and state energies of model chromophores without counterion. This material is available free of charge via the Internet at <http://pubs.acs.org>.

## References and Notes

- (1) Palings, I.; Pardo, J. A.; van den Berge, E.; Winkel, C.; Lugtenburg, J.; Mathies, R. A. *Biochemistry* **1987**, *26*, 2544.
- (2) Menon, S. T.; Han, M.; Sakmar, T. P. *Physiol. Rev.* **2001**, *81*, 1659.
- (3) Okada, T.; Ernst, O. P.; Palczewski, K.; Hofmann, K. P. *Trends Biochem. Sci.* **2001**, *26*, 318.
- (4) Palczewski, K.; Kumasaka, T.; Hori, T.; Behnke, C. A.; Motoshima, H.; Fox, B. A.; Le Trong, I.; Teller, D. C.; Okada, T.; Stenkamp, R. E.; Yamamoto, M.; Miyano, M. *Science* **2000**, *289*, 739.
- (5) Okada, T.; Fujiyoshi, Y.; Silow, M.; Navarro, J.; Landau, E. M.; Shichida, Y. *Proc. Natl. Acad. Sci. U.S.A.* **2002**, *99*, 5982.
- (6) Okada, T.; Sugihara, M.; Bondar, A.-N.; Elstner, M.; Entel, P.; Buss, V. *J. Mol. Biol.* **2004**, *342*, 571.
- (7) Lythgoe, J. N.; Vertebrate Visual Pigments. In *Handbook of Sensory Physiology*; Dartnall, H. J. A., Ed.; Springer: New York, 1972; Vol. 7, p 605.
- (8) Shichi, H. *Biochemistry of Vision*; Academic Press: New York, 1983.
- (9) deGrip W. J.; Rothschild, K. J. Structure and Mechanism of Vertebrate Visual Pigments. In *Handbook of Biological Physics*; Stavenga,
- (10) Irving, C. S.; Vyders, G. W.; Leermakers, P. A. *J. Am. Chem. Soc.* **1969**, *91*, 2141.
- (11) Birge, R. R.; Schulten, K.; Karplus, M. *Chem. Phys. Lett.* **1975**, *31*, 451.
- (12) Honig, B.; Dinur, U.; Nakanishi, K.; Balogh-Nair, V.; Gawinowicz, M. A.; Arnaboldi, M.; Motto, M. G. *J. Am. Chem. Soc.* **1979**, *101*, 7084.
- (13) Schulten, K.; Dinur, U.; Honig, B. *J. Chem. Phys.* **1980**, *73*, 3927.
- (14) Raudino, A.; Zuccarello, F.; Buemi, G. *J. Chem. Soc., Faraday Trans.* **1983**, *79*, 1759.
- (15) Hu, J.; Griffin, R. G.; Herzfeld, J. *Proc. Natl. Acad. Sci. U.S.A.* **1994**, *91*, 8880.
- (16) Kusnetzow, A.; Singh, D. L.; Martin, C. H.; Barani, I. J.; Birge, R. R. *Biophys. J.* **1999**, *76*, 2370.
- (17) Tajkhorshid, E.; Suhai, S. *Theor. Chem. Acc.* **1999**, *101*, 180.
- (18) Hayashi, S.; Ohmine, I. *J. Phys. Chem. B* **2000**, *104*, 10678.
- (19) Hayashi, S.; Tajkhorshid, E.; Pebay-Peyroula, E.; Royant, A.; Landau, E. M.; Navarro, J.; Schulten, K. *J. Phys. Chem. B* **2001**, *105*, 10124.
- (20) Kusnetzow, A.; Dukkpati, A.; Babu, K. R.; Singh, D.; Vought, B. W.; Knox, B. E.; Birge, R. R. *Biochemistry* **2001**, *40*, 7832.
- (21) Ren, L.; Martin, C. H.; Wise, K. J.; Gillespie, N. B.; Luecke, H.; Lanyi, J. K.; Spudich, J. L.; Birge, R. R. *Biochemistry* **2001**, *40*, 13906.
- (22) Houjou, H.; Inoue, Y.; Sakurai, M. *J. Phys. Chem. B* **2001**, *105*, 867.
- (23) Rajamani, R.; Gao, J. *J. Comput. Chem.* **2002**, *23*, 97.
- (24) Vreven, T.; Morokuma, K. *Theor. Chem. Acc.* **2003**, *109*, 125.
- (25) Ferré, N.; Olivucci, M. *J. Am. Chem. Soc.* **2003**, *125*, 6868.
- (26) Schreiber, M.; Buss, V. *Int. J. Quantum Chem.* **2003**, *95*, 882.
- (27) Schreiber, M.; Buss, V.; Sugihara, M. *J. Chem. Phys.* **2003**, *119*, 12045.
- (28) Buss, V.; Sugihara, M.; Entel, P.; Hafner, J. *Angew. Chem., Int. Ed.* **2003**, *42*, 3245.
- (29) Sugihara, M.; Buss, V.; Entel, P.; Hafner, J. *J. Phys. Chem. B* **2004**, *108*, 3673.
- (30) Kresse, G.; Furthmüller, J. *Phys. Rev. B* **1996**, *54*, 11169.
- (31) Sugihara, M.; Buss, V.; Entel, P.; Elstner, M.; Frauenheim, T. *Biochemistry* **2002**, *41*, 15259.
- (32) Andersson, K.; Baryz, M.; Bernhardsson, A.; Blomberg, M. R. A.; Cooper, D. L.; Fülcher, M. P.; de Graaf, C.; Hess, B.; Karlström, G.; Lindh, R.; Malmqvist, P.-Å.; Nakajima, T.; Neogrady, P.; Olsen, J.; Roos, B. O.; Schimmelpfennig, B.; Schütz, M.; Seijo, L.; Serrano-Andres, L.; Siegbahn, P. E.; Ståhring, J.; Thorsteinsson, T.; Veryazov, V.; Widmark, P.-O. *Molcas*, Version 5.4; Department of Theoretical Chemistry, Chemistry Center, University of Lund: Lund, Sweden, 2002.
- (33) Anderson, K.; Malmqvist, P.-Å.; Roos, B. O.; Sadlej, A. J.; Wolinski, K. *J. Phys. Chem.* **1990**, *94*, 5483.
- (34) Anderson, K.; Malmqvist, P.-Å.; Roos, B. O. *J. Chem. Phys.* **1992**, *96*, 1218.
- (35) Widmark, P.-O.; Malmqvist, P.-Å.; Roos, B. O. *Theor. Chim. Acta* **1990**, *77*, 291.
- (36) Pierloot, K.; Dumez, B.; Widmark P.-O.; Roos, B. O. *Theor. Chim. Acta* **1995**, *90*, 87.
- (37) Schreiber, M.; Buss, V.; Fülcher, M. P. *J. Phys. Chem. Chem. Phys.* **2001**, *3*, 3906.
- (38) Schreiber, M.; Buss, V. *J. Phys. Chem. Chem. Phys.* **2002**, *4*, 3305.
- (39) Malmqvist, P.-Å.; Roos, B. O. *Chem. Phys. Lett.* **1989**, *155*, 189.
- (40) Schoenlein, R. W.; Peteanu, L. A.; Mathies, R. A.; Shank C. V. *Science* **1991**, *254*, 412.
- (41) Garavelli, M.; Bernardi, F.; Olivucci, M.; Vreven, T.; Klein, S.; Celani, P.; Robb, M. A. *Faraday Discuss.* **1998**, *110*, 51.
- (42) Buss, V.; Weingart, O.; Sugihara, M. *Angew. Chem., Int. Ed.* **2000**, *39*, 2784.
- (43) Bifone, A.; de Groot, H. J. M.; Buda, F. *J. Phys. Chem. B* **1997**, *101*, 2954.
- (44) Buda, F.; Giannozzi, P.; Mauri, F. *J. Phys. Chem. B* **2000**, *104*, 9048.
- (45) Teller, D. C.; Okada, T.; Behnke, C. A.; Palczewski, K.; Stenkamp, R. E. *Biochemistry* **2001**, *40*, 7761.
- (46) Mebane, A. D. *J. Am. Chem. Soc.* **1952**, *74*, 5227.
- (47) Serrano-Andrés, L.; Lindh, R.; Roos, B. O.; L.; Merchán, M. *J. Phys. Chem.* **1993**, *97*, 9360.
- (48) Mathies R.; Stryer, L. *Proc. Natl. Acad. Sci. U.S.A.* **1976**, *73*, 2169.
- (49) Ponder, M.; Mathies, R. *J. Phys. Chem.* **1983**, *87*, 5090.
- (50) Yan, E. C.; Kazmi, M. A.; Ganim, Z.; Hou, J. M.; Pan, D.; Chang, B. S. W.; Sakmar, T. P.; Mathies, R. A. *Proc. Natl. Acad. Sci. U.S.A.* **2003**, *100*, 9262.
- (51) Birge, R. R.; Knox, B. E. *Proc. Natl. Acad. Sci. U.S.A.* **2003**, *100*, 9105.
- (52) Warshel, A. *Proc. Natl. Acad. Sci. U.S.A.* **1978**, *75*, 2558.

- (53) Steinberg, G.; Ottolenghi, M.; Sheves, M. *Biophys. J.* **1993**, 84, 1499.
- (54) Terstegen, F.; Buss, V. *J. Mol. Struct. (THEOCHEM)* **1996**, 369, 53.
- (55) Ferré, N.; Cembran, A.; Garavelli, M.; Olivucci, M. *Theor. Chem. Acc.* **2004**, 112, 335.

- (56) Carravetta, M.; Zhao, X.; Johannessen, O. G.; Lai, W. C.; Verhoeven, M. A.; Bovee-Geurths, P. H. M.; Verdegem, P. J. E.; Kiihne, S.; Luthaman, H.; de Groot, H. J. M.; deGrip, W. J.; Lugtenburg, J.; Levitt, M. H. *J. Am. Chem. Soc.* **2004**, 126, 3948.
- (57) Touw, S. I. E.; de Groot, H. J. M.; Buda, F. *J. Phys. Chem. B* **2004**, 108, 13560.